

Channel-resolved subcycle interferences of electron wave packets emitted from H_2 in two-color laser fields

Xinhua Xie,^{*} Stefan Roither, Daniil Kartashov, Li Zhang, Andrius Baltuška, and Markus Kitzler
Photonics Institute, Vienna University of Technology, Gusshausstrasse 27, A-1040 Vienna, Austria

We report on the observation of subcycle interferences of electron wave packets released during the strong field ionization of H_2 with cycle-shaped two-color laser fields. With a reaction microscope, channel-resolved photoelectron momentum distribution are obtained for different final products originating from single ionization of H_2 . Our results show that the subcycle interference structures of electron wave packet are very sensitive to the cycle-shape of the two-color laser field. The reason is that the ionization time within an optical cycle is determined by the cycle-shape of the laser field. The subcycle interference structures can be further used to get the subcycle dynamics of molecules during strong field interaction.

I. INTRODUCTION

Both electronic and nuclear vibrational dynamics play a crucial role in molecular reactions, such as molecular ionization, dissociation and isomerization [1]. In general, nuclear vibrational dynamics happens on time scales from tens of femtosecond up to hundreds of femtosecond, while the valence electronic dynamics takes place on the sub-femtosecond/attosecond time scale [2]. Therefore, techniques with attosecond temporal resolution are required to gain insight into the dynamics of valence electrons in molecules. Experimental techniques such as attosecond extreme-ultraviolet or x-ray transient absorption spectroscopy [3–6], high harmonic spectroscopy [7–9], and photoelectron spectroscopy based on electron wave packet (EWP) interferences [10–15], have been demonstrated in studies of attosecond electronic dynamics in atoms and molecules [16]. To retrieve the motion of valence electrons in a molecule, not only attosecond temporal resolution is required but also information on the involved molecular orbitals and the geometry of the molecule is critical. Since the EWPs released during tunneling ionization of molecules carry phase information on the molecular orbital where they are emitted from [17], this information can be retrieved from the interference patterns of EWPs in photoelectron spectra. In the past years, EWP interferometry has been applied in studies of ionization dynamics [12], the molecular orbital [18], and the influence of the ionic Coulomb potential [11, 19]. The phase of the interfering EWPs can be reconstructed, and dynamical information taking place during the strong field interaction can be read out from the interference pattern with attosecond temporal resolution [12].

Four types of strong-field-induced EWP interferences in molecules can be distinguished: The first type are the inter-cycle interferences (ICI) produced by EWPs released during different optical cycles which lead to ATI (above-threshold ionization)-like structures in the momentum or the energy distribution of photoelectrons

[13, 20]. The second type are the so-called subcycle interferences (SCI) formed by EWPs detached during different half cycles within one optical cycle [12, 21–23]. The third type of interferences are formed by EWPs removed from the system during the same quarter of one optical cycle due to scattering on the ionic potential [11, 24, 25]. The fourth type are multi-center interferences due to EWPs scattering on different nuclei of a molecule [24, 26]. Accurately defined momentum-to-time mapping and a precise identification of the type of observed interference fringes is necessary for retrieving the information of electronic dynamics and structures from the measured interference pattern. Previous studies reveal that it is important to consider the influence of the ionic Coulomb potential [11, 12, 19, 27]. However, this is not a trivial task. Besides, because of the mixture of different kind of interferences and complicated low-energy structures (LES) [28–31], the fringe positions will be modified which affects the precision of the phase reconstruction [20].

To obtain a well-defined interference pattern of EWPs, a cycle-shaped laser field is beneficial, because the EWP interference pattern are induced by EWPs released at different time. Their release time is this extremely sensitive to the shape of the laser field and can be controlled by the cycle shape of the laser field. There are several ways to obtain such laser fields. One of the most straightforward methods is to stabilize the carrier-envelope phase of a few-cycle laser pulse. Another method is to lock the phase delay between multiple laser fields with different colors. Such cycle-shaped laser fields have already been applied in studies of controlling high harmonic generation [32, 33], molecular orientation [34] and dissociation [35], and single and double ionization of atoms [12, 27, 36].

In this work, we employed a two-color laser field with precise control on the relative phase between a fundamental laser field and its second harmonic. In a previous study [12], we have demonstrated that subcycle ionization dynamics can be retrieved from the SCI patterns of atomic targets created by such two-color laser fields. It has been shown that with a cycle-shaped two-color laser field the final momentum of electrons can be shifted to bigger momentum values to avoid overlapping with the complex LES and to minimize influence from

^{*} Electronic address: xinhua.xie@tuwien.ac.at

the Coulomb potential [12].

In case of molecules, because of small differences in the ionization potentials and different angular dependence of ionization rates, tunnel ionization may happen from lower lying molecular orbitals rather than the HOMO [37]. Moreover, the strong field interaction may lead to dissociation of the molecule along different pathways [38]. To get access to the electron dynamics of molecular ionization, discrimination between these different pathways is necessary. Here we extend the application of using subcycle EWP interferometry from atoms to molecules with coincidence measurements which allows disentangling measured the different contributions of pathways to the interference structures. For our proof-of-principle measurements we chose the simplest molecule, hydrogen (H_2), as the target.

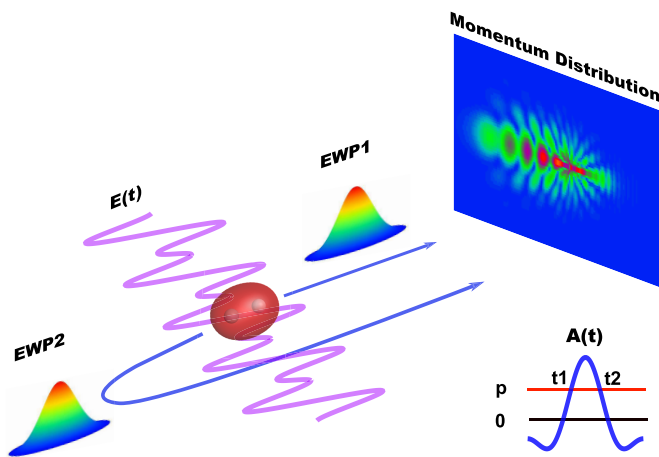


FIG. 1. A schematic view of subcycle EWP interferences. When a molecule is exposed to a two-color laser field, shown as the magenta line, EWPs will be released around the field's peaks. In a unit cell of the pulse, the EWPs released during each half cycle (t_1 and t_2) will lead to the same final momentum p , which lead to interference fringes in the momentum space.

A schematic view of subcycle EWP interference is shown in Fig. 1. The EWPs released at different times within one laser optical cycle may end at the same final momentum and therefore interfere with each other in the momentum space. Measurement of the photoelectron momentum distribution with a reaction microscope allows recording these interferences [39, 40].

II. EXPERIMENTS

Coincidence measurements of electrons and ions were performed for H_2 with a reaction microscope. A laser beam from a home-built Ti:Sapphire laser amplifier system with a center wavelength of 795 nm, a repetition rate of 5 kHz and a pulse duration (full width at half maximum of the intensity) of about 25 fs is superim-

posed with the second harmonic beam generated by a 500 μm type-I BBO crystal. The pulse duration of the second harmonic pulse is 46 fs according to self diffraction measurements. The second harmonic beam is polarized parallel to the fundamental beam and the peak laser intensities are about $6 \times 10^{13} \text{ W/cm}^2$ for each beam. The group velocity delay between the two laser beams were compensated by calcite plates and a pair of fused silica wedges which was also used to adjust the phase delay between the two colors in steps of 0.06π . The calibration of the relative phase between the two colors and the laser peak intensities is performed from measurements of helium, as described in Ref.[12]. A weak homogeneous dc field of 2.5 V/cm is applied along the time-of-flight (TOF) spectrometer to accelerate electrons and ions towards two position-sensitive multi-channel plate detectors. Additionally, a homogeneous magnetic field of 6.4 gauss ensures 4π detection of electrons. The beam of hydrogen molecules with a diameter of about 170 μm is prepared by supersonic expansion through a nozzle with a diameter of 30 μm and collimated with a two-stage skimmer before the ultra-high vacuum interaction chamber (about 1.3×10^{-10} mbar). TOFs and positions of electrons and ions are recorded and the momentum vectors of all particles are retrieved in the off-line data analysis. Momentum conservation condition between electrons and ions can be applied to achieve coincidence selection to minimize the background signals. To ensure a high efficiency of coincidence detection, the ionization rate is kept at about 0.4 ionization events per laser shot. More details on the experimental setup can be found in our previous publications [12, 38].

III. RESULTS AND DISCUSSION

A. H_2 in two-color laser fields

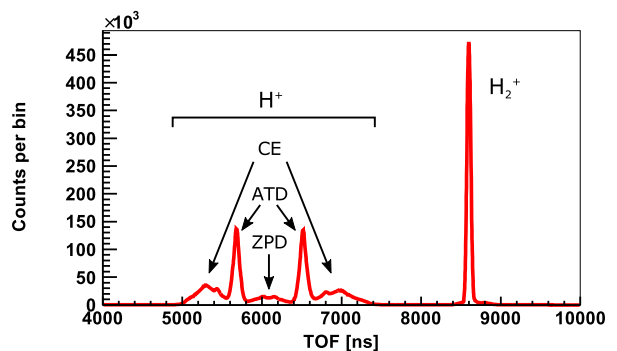


FIG. 2. Time-of-flight spectrum of H_2 interacting with two-color laser fields. In the H^+ distribution, there are three regions: zero-photon-dissociation (ZPD), above-threshold-dissociation (ATD) and Coulomb explosion (CE).

When a hydrogen molecule interacts with a strong laser

field, one electron can be removed through tunnel ionization. After single ionization, the molecule will reach a cationic state. H_2^+ may then dissociate into a proton and a hydrogen atom, or H_2^+ can be further ionized and eventually lead to Coulomb explosion into two protons. A typical time-of-flight spectrum of H_2 in a strong two-color laser field is presented in Fig. 2. The single ionization (H_2^+), dissociation ($\text{H}^+ + \text{H}$) and Coulomb explosion ($\text{H}^+ + \text{H}^+$) pathways can be well distinguished. As marked in Fig. 2, there are two pathways for the dissociation of H_2^+ : above-threshold dissociation (ATD) leading to protons with high energy, and zero-photon dissociation (ZPD) leading to low-energy protons [41, 42].

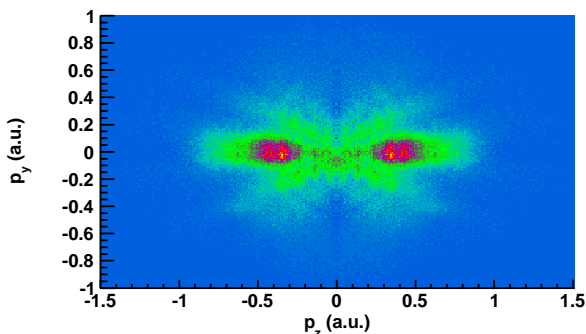


FIG. 3. A slice through a measured electron momentum distribution in the $x-z$ plane (laser field polarization along z -direction) with a condition $|p_y| < 0.1 \text{ a.u.}$ and integration over all relative phases. Momentum conservation conditions between one electron and H_2^+ is applied to the measured data to ensure coincidence selection. To enhance the visibility of structures induced by electron wave packet interferences, a gaussian function is subtracted for each relative phase.

First we focus on the single ionization leading to H_2^+ . A measured electron momentum distribution correlated with H_2^+ is shown in Fig. 3, integrated over all relative two-color phases. In the distribution there are two clear types of structures: finger-like patterns due to scattering of EWPs on the parent nucleus and ATI-like ring structures. Here in this paper, we focus on SCI of EWPs released during strong field interaction. However, in Fig. 3, there are no clear structures of subcycle EWP interference. The reason is that the subcycle EWP interference is very sensitive to the cycle shape of the laser field. As the electron momentum distribution in Fig. 3 is integrated over all relative phases between the two color fields, the structure of SCI is smeared out.

B. Photoelectron momentum distribution over relative phase

Measured distributions of the H_2^+ ionic momentum along the laser polarization direction (p_z) over the relative phase are shown in Fig. 4(a). Clear 2π -periodic

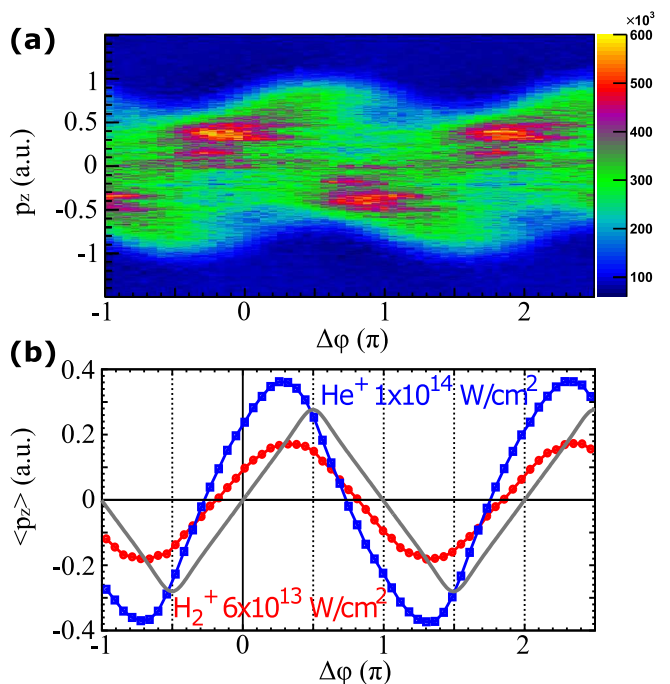


FIG. 4. (a) Measured ion momentum distribution along the laser polarization direction over the relative phase between the two colors. To enhance the visibility of structures induced by electron wave packet interferences, a gaussian function is subtracted for each relative phase. (b) The mean value of the momentum distribution along the laser polarization direction as a function of the relative phase between the two colors. The gray line represents the simulated results using SFA.

modulations can be seen. The mean momentum value oscillates over the relative phase [depicted in Fig. 4(b) as red circles] and reaches maximum offset at $\Delta\phi = 0.35 + n\pi, n \in \mathbb{Z}$. The mean value of the momentum distribution is determined by the shape of the laser field vector potential. For relative phase 0, the vector potential of the two-color field is symmetric, which according to prediction of the simple-man's model within the strong field approximation (SFA) [43] should lead to zero mean value. As shown previously, the observed offset from 0 is due to the ionic Coulomb potential [19, 44, 45]. The phase shift due the Coulomb potential is about -0.2π as compared with the simple-man's results, in which the Coulomb effect is neglected [44, 45]. The momentum mean value of a measurement on helium with higher laser peak intensity ($1 \times 10^{13} \text{ W/cm}^2$ for each color) [12] is plotted in Fig. 4(b) as blue squares. The amplitude of the mean value oscillation for helium is almost twice as that for hydrogen because of the higher peak laser intensity. On the other hand, we notice that the phase shift of the helium measurements is about -0.3π , i.e. more than that of the hydrogen measurement. This contradicts our previous finding that the Coulomb effect is stronger for lower laser peak intensity [19]. The reason may be the participation of excited states or non-adiabatic effects in the

ionization process [46, 47].

C. Subcycle interference of electron wave packet

To observe SCI structures we investigate electron momentum distributions for certain relative phases between the two colors, since for electrons the momentum resolution is much higher along the directions perpendicular to the laser polarization direction than for ions. The measured electron momentum distribution in the laser polarization plane is illustrated in Fig. 5(f-j) for five different relative phases (0, 0.25π , 0.5π , 0.75π and π). The structures in the momentum distribution look similar to those measured for helium [12]. There are sharp ATI-like peaks in the low momentum region as shown in the p_z distribution [Fig. 5(k-o)] and finger-like structures in the 2D momentum distribution [Fig. 5(f-j)]. SCI structures can be seen in the 1D momentum distribution as big humps [Fig. 5(k-o)]. However, in details the distributions are different from those observed for helium because of different laser intensities, different ionic potential and energy structure.

First, we focus on the results with relative phase 0. According to the shape of the vector potential [Fig. 5(a)], the momentum distribution should be symmetric along z -direction. However, due to the Coulomb effect, the EWP released before the peak will be driven back and scatter with the parent ion which leads to the appearance of clear finger-like holographic structures. In the results for helium, there are no obvious SCI structures. The reason is that for helium the ionization mainly happens near the major peak within one optical cycle and therefore the SCI of EWPs is suppressed. In contrast, for H_2^+ there appear SCI fringes for $p_z > 0.2$ a.u. in the momentum distribution [Fig. 5(f,k)]. Such a structure within the SFA is induced by the interference of EWPs released at t_1 , the minor peak within one optical cycle, and t_2 , before the major peak. EWPs released at t_1 and t_2 end at the same final momentum and lead to SCI. The reason for the more pronounced SCI structure for a relative phase of 0 in hydrogen than in helium may be the following: The ionization potential of helium, 24.6 eV, is higher than that of hydrogen, 15.5 eV. Therefore, the ionization of helium dominantly happens near the main peak within a laser optical cycle, while in the ionization of hydrogen the two minor peaks may have also contribute considerably.

For a relative phase of 0.5π , the laser electric field is symmetric [Fig. 5(c)]. Therefore, within one optical cycle, ionization may happen equally at the two main peaks (t_1 and t_2) and the released EWPs will interfere with each other in the momentum space because they will end at the same final momentum. In Ref. [12], the SCI with observed at a relative phase 0.5π is applied to retrieve the phase of the released EWPs and to investigate the electron dynamics during strong field ionization. As shown in Fig. 5(h), there are clear SCI structure on the negative momentum side.

When the relative phase between the two colors varies, the cycle structure of the laser field varies accordingly. Since tunneling ionization is very sensitive to the field strength of a laser field. Therefore, the ionization time within an optical cycle can be well controlled with the laser cycle shape and leads to the control of SCI. As presented in Fig. 5, it is clearly shown that the interference structures, especially the SCI structures, strongly depend on the relative phase of the two colors.

D. Subcycle interference of electron wave packet for dissociation pathways

After single ionization in a two-color field, H_2^+ may dissociate into a proton and a hydrogen atom through ATD or ZPD. We can distinguish the dissociation pathways based on the kinetic energy release during the dissociation process. By coincidence gating we can obtain the corresponding photoelectron spectra. From the channel-resolved photoelectron spectra we can get access to the electron and nuclear dynamics which leads to the certain dissociation channels. For H_2 the different channels can be easily separated by the proton momentum. We select the proton momentum in the range of $6 < |p_z| < 11$ a.u. for ATD, and $|p_z| < 6$ a.u. for ZPD.

In Fig. 6 electron momentum distributions along the laser polarization direction are plotted for the ATD pathway and a relative phase of 0. The structure is similar to that of the H_2^+ pathway [Fig. 5(f)]. Due to the limited momentum resolution, further comparison in detail is not meaningful for this measurement. Our experimental observation of SCI in the strong field ionization of H_2 constitutes a proof-of-principle experiment of channel-resolved EWP interferometry based on SCI. Similarly to channel-resolve ATI spectroscopy based on the ICI of EWPs [13], channel-resolved subcycle EWP interferometry can be applied to investigate the relation between electron dynamics and nuclear dynamics in molecules induced by strong field interaction.

IV. CONCLUSION

In conclusion, we demonstrated a proof-of-principle experiment of channel-resolved EWP interferometry based on SCI of EWP released during strong field interaction. We report on the observation of SCI in the strong field interaction of hydrogen molecules with cycle-shaped two-color laser fields. It is found that the structure of SCI is very sensitive to the cycle shape of the two-color laser fields. Because in the measurement ATD and ZPD of H_2^+ can be distinguished with proton energy, channel-resolved electron momentum spectra could be obtained for the ionization and dissociation channel for H_2^+ . The channel-resolved subcycle EWP interferometry demonstrated here can be employed for studies of multi-electron

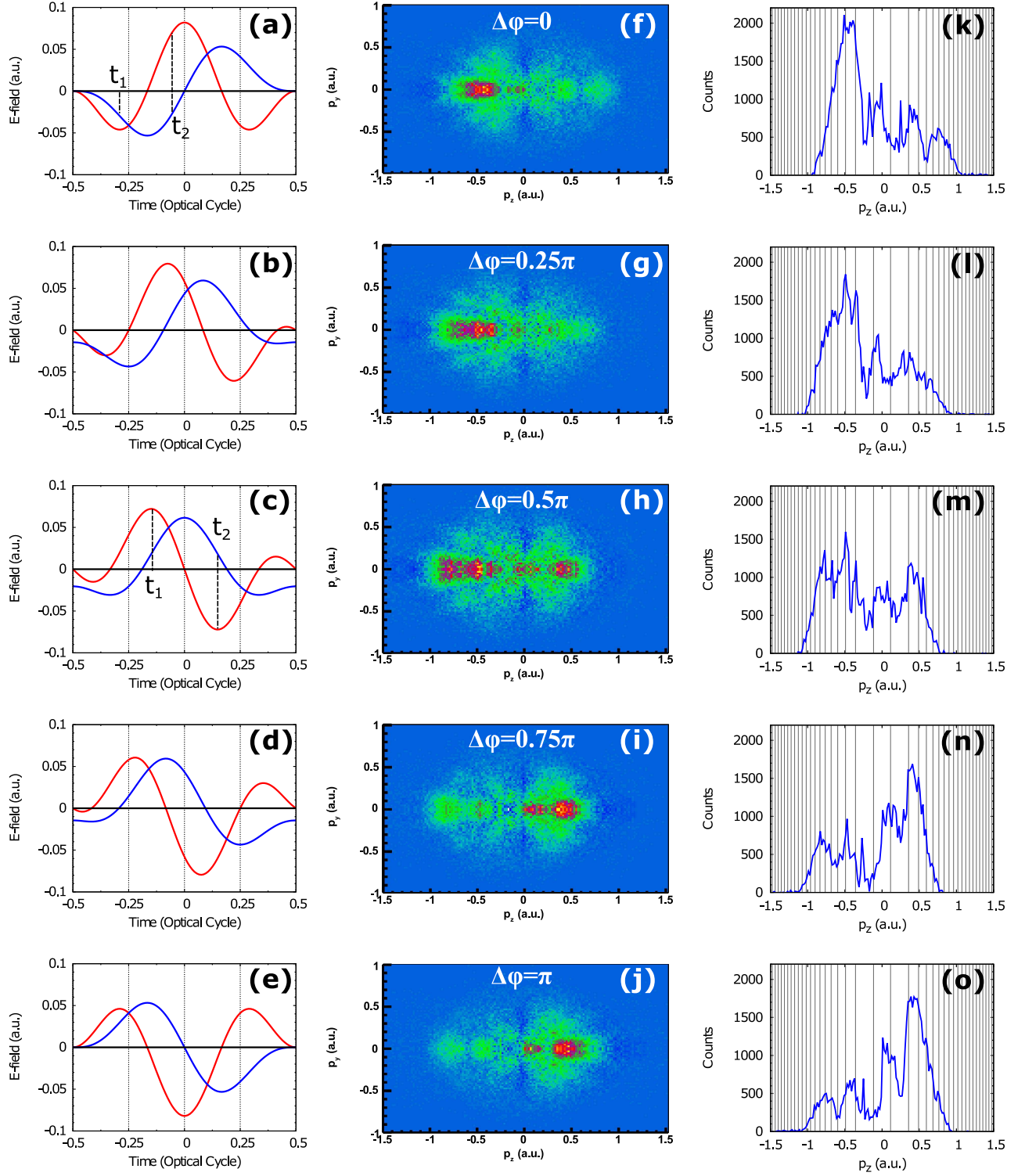


FIG. 5. (a-e) Electric fields (red lines) and vector potentials (blue lines) for relative phases 0, 0.25π , 0.5π , 0.75π and π . (f-j) Measured electron momentum distributions in the laser polarization plane with subtraction of a gaussian function for the five relative phases. (k-o) Momentum distributions along the laser polarization direction with $|p_{x,y}| < 0.1$ a.u. for the five relative phases. Vertical gray lines indicate the positions of the ATI peaks.

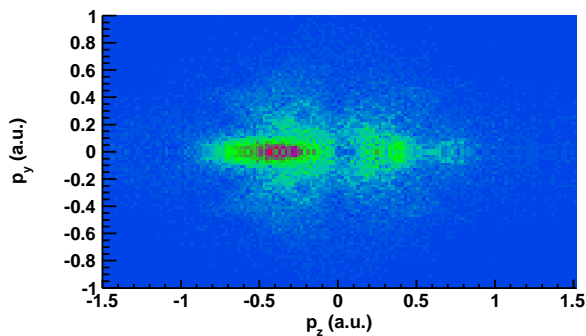


FIG. 6. Electron momentum distribution for a relative phase of 0 for the ATD pathway.

and multi-orbital effects in the laser field-induced ionization and dissociation of molecules [13, 48, 49].

V. ACKNOWLEDGEMENT

This research was financed by the Austrian Science Fund (FWF) under grants P25615-N27, P28475-N27, P21463-N22, P27491-N27, and SFB-F49 NEXTlite, and by a starting grant from the European Research Council (ERC project CyFi).

-
- [1] Kaoru Yamanouchi. The Next Frontier. *Science*, 295(5560):1659–1660, 2002.
 - [2] Predrag Ranitovic, Craig W. Hogle, Paula Riviere, Alicia Palacios, Xiao-Ming Tong, Nobuyuki Toshima, Alberto Gonzalez-Castrillo, Leigh Martin, Fernando Martn, Margaret M. Murnane, and Henry Kapteyn. Attosecond vacuum uv coherent control of molecular dynamics. *Proceedings of the National Academy of Sciences*, 111(3):912–917, 2014.
 - [3] Eleftherios Goulielmakis, Zhi-Heng Loh, Adrian Wirth, Robin Santra, Nina Rohringer, Vladislav S. Yakovlev, Sergey Zherebtsov, Thomas Pfeifer, Abdallah M. Azzeer, Matthias F. Kling, Stephen R. Leone, and Ferenc Krausz. Real-time observation of valence electron motion. *Nature*, 466(7307):739–743, 2010.
 - [4] He Wang, Michael Chini, Shouyuan Chen, Chang-Hua Zhang, Feng He, Yan Cheng, Yi Wu, Uwe Thumm, and Zenghu Chang. Attosecond time-resolved autoionization of argon. *Phys. Rev. Lett.*, 105:143002, 2010.
 - [5] Michael Chini, Baozhen Zhao, He Wang, Yan Cheng, S. X. Hu, and Zenghu Chang. Subcycle ac stark shift of helium excited states probed with isolated attosecond pulses. *Phys. Rev. Lett.*, 109:073601, 2012.
 - [6] Zhi-Heng Loh and Stephen R. Leone. Capturing ultrafast quantum dynamics with femtosecond and attosecond x-ray core-level absorption spectroscopy. *The Journal of Physical Chemistry Letters*, 4(2):292–302, 2013.
 - [7] Olga Smirnova, Yann Mairesse, Serguei Patchkovskii, Nirit Dudovich, David Villeneuve, Paul Corkum, and Misha Y. Ivanov. High harmonic interferometry of multi-electron dynamics in molecules. *Nature*, 460:972–977, 2009.
 - [8] AD Shiner, BE Schmidt, C Trallero-Herrero, HJ Wörner, S Patchkovskii, PB Corkum, JC Kieffer, F Légaré, and DM Villeneuve. Probing collective multi-electron dynamics in xenon with high-harmonic spectroscopy. *Nature Physics*, 7(6):464–467, 2011.
 - [9] HJ Wörner, JB Bertrand, B Fabre, J Higuier, H Ruf, A Dubrouil, S Patchkovskii, M Spanner, Y Mairesse, Valérie Blanchet, et al. Conical intersection dynamics in no2 probed by homodyne high-harmonic spectroscopy. *Science*, 334(6053):208–212, 2011.
 - [10] R. Gopal, K. Simeonidis, R. Moshhammer, Th. Ergler, M. Dürr, M. Kurka, K.-U. Kühnel, S. Tschuch, C.-D. Schröter, D. Bauer, J. Ullrich, A. Rudenko, O. Herrwerth, Th. Uphues, M. Schultze, E. Goulielmakis, M. Uiberacker, M. Lezius, and M. F. Kling. Three-dimensional momentum imaging of electron wave packet interference in few-cycle laser pulses. *Phys. Rev. Lett.*, 103(5):053001, 2009.
 - [11] Y. Huismans, A. Rouzée, A. Gijsbertsen, J. H. Jungmann, A. S. Smolkowska, P. S. W. M. Logman, F. Lépine, C. Cauchy, S. Zamith, T. Marchenko, J. M. Bakker, G. Berden, B. Redlich, A. F. G. van der Meer, H. G. Muller, W. Vermin, K. J. Schafer, M. Spanner, M. Y. Ivanov, O. Smirnova, D. Bauer, S. V. Popruzhenko, and M. J. J. Vrakking. Time-Resolved Holography with Photoelectrons. *Science*, 331:61–, 2011.
 - [12] Xinhua Xie, Stefan Roither, Daniil Kartashov, Emil Persson, Diego G. Arbó, Li Zhang, Stefanie Gräfe, Markus S. Schöffler, Joachim Burgdörfer, Andrius Baltuska, and Markus Kitzler. Attosecond probe of valence-electron wave packets by subcycle sculpted laser fields. *Phys. Rev. Lett.*, 108:193004, 2012.
 - [13] Andrey E. Boguslavskiy, Jochen Mikosch, Arjan Gijsbertsen, Michael Spanner, Serguei Patchkovskii, Niklas Gador, Marc J. J. Vrakking, and Albert Stolow. The Multielectron Ionization Dynamics Underlying Attosecond Strong-Field Spectroscopies. *Science*, 335(6074):1336–1340, 2012.
 - [14] Lucas J. Zipp, Adi Natan, and Philip H. Bucksbaum. Probing electron delays in above-threshold ionization. *Optica*, 1(6):361–364, 014.
 - [15] Xinhua Xie. Two-Dimensional Attosecond Electron Wave-Packet Interferometry. *Physical Review Letters*, 114(17):173003, 2015.
 - [16] Ferenc Krausz and Misha Ivanov. Attosecond physics. *Rev. Mod. Phys.*, 81(1):163–234, 2009.
 - [17] Xinhua Xie, Gerald Jordan, Marlene Wickenhauser, and Armin Scrinzi. Time and momentum distributions of rescattering electrons. *Journal of Modern Optics*, 54(7):999–1010, 2007.
 - [18] M. Meckel, D. Comtois, D. Zeidler, A. Staudte, D. Pavicic, H. C. Bandulet, H. Pepin, J. C. Kieffer, R. Dörner,

- D. M. Villeneuve, and P. B. Corkum. Laser-induced electron tunneling and diffraction. *Science*, 320(5882):1478–1482, 2008.
- [19] Xinhua Xie, Stefan Roither, Stefanie Gräfe, Daniil Kartashov, Emil Persson, Christoph Lemell, Li Zhang, Markus S Schöffler, Andrius Baltuška, Joachim Burgdörfer, Others, Andrius Baltuška, and Markus Kitzler. Probing the influence of the Coulomb field on atomic ionization by sculpted two-color laser fields. *New Journal of Physics*, 15(4):43050, 2013.
- [20] Diego G. Arbó, Kenichi L. Ishikawa, Klaus Schiessl, Emil Persson, and Joachim Burgdörfer. Diffraction at a time grating in above-threshold ionization: The influence of the coulomb potential. *Phys. Rev. A*, 82(4):043426, 2010.
- [21] F. Lindner, M. G. Schätzel, H. Walther, A. Baltuška, E. Goulielmakis, F. Krausz, D. B. Milošević, D. Bauer, W. Becker, and G. G. Paulus. Attosecond double-slit experiment. *Phys. Rev. Lett.*, 95(4):040401, 2005.
- [22] Diego G. Arbó, Emil Persson, and Joachim Burgdörfer. Time double-slit interferences in strong-field tunneling ionization. *Phys. Rev. A*, 74(6):063407, 2006.
- [23] Diego G. Arbó, Stefan Nagele, Xiao-Min Tong, Xinhua Xie, Markus Kitzler, and Joachim Burgdörfer. Interference of electron wave packets in atomic ionization by subcycle sculpted laser pulses. *Phys. Rev. A*, 89:043414, 2014.
- [24] Michael Spanner, Olga Smirnova, Paul B Corkum, and Misha Yu Ivanov. Reading diffraction images in strong field ionization of diatomic molecules. *Journal of Physics B: Atomic, Molecular and Optical Physics*, 37(12):L243, 2004.
- [25] Xue-Bin Bian and André Bandrauk. Attosecond Time-Resolved Imaging of Molecular Structure by Photoelectron Holography. *Physical Review Letters*, 108(26):1–4, 2012.
- [26] S N Yurchenko, S Patchkovskii, I V Litvinyuk, P B Corkum, and G L Yudin. Laser-Induced Interference, Focusing, and Diffraction of Rescattering Molecular Photoelectrons. *Phys. Rev. Lett.*, 93(22):223003, 2004.
- [27] Li Zhang, Xinhua Xie, Stefan Roither, Daniil Kartashov, YanLan Wang, ChuanLiang Wang, Markus Schöffler, Dror Shafir, Paul B. Corkum, Andrius Baltuška, Igor Ivanov, Anatoli Kheifets, XiaoJun Liu, André Staudte, and Markus Kitzler. Laser-sub-cycle two-dimensional electron-momentum mapping using orthogonal two-color fields. *Phys. Rev. A*, 90:061401, 2014.
- [28] C. I. Blaga, F. Catoire, P. Colosimo, G. G. Paulus, H. G. Muller, P. Agostini, and L. F. DiMauro. Strong-field photoionization revisited. *Nature Physics*, 5(5):335–338, 2009.
- [29] W. Quan, Z. Lin, M. Wu, H. Kang, H. Liu, X. Liu, J. Chen, J. Liu, X. T. He, S. G. Chen, H. Xiong, L. Guo, H. Xu, Y. Fu, Y. Cheng, and Z. Z. Xu. Classical aspects in above-threshold ionization with a midinfrared strong laser field. *Phys. Rev. Lett.*, 103:093001, 2009.
- [30] Chengpu Liu and Karen Z. Hatsagortsyan. Origin of unexpected low energy structure in photoelectron spectra induced by midinfrared strong laser fields. *Phys. Rev. Lett.*, 105:113003, 2010.
- [31] D. Dimitrovski, J. Maurer, H. Stapelfeldt, and L. B. Madsen. Low-energy photoelectrons in strong-field ionization by laser pulses with large ellipticity. *Phys. Rev. Lett.*, 113:103005, 2014.
- [32] E Goulielmakis, M Schultze, M Hofstetter, V S Yakovlev, J Gagnon, M Uiberacker, a L Aquila, E M Gullikson, D T Attwood, R Kienberger, F Krausz, and U Kleineberg. Single-cycle nonlinear optics. *Science*, 320(5883):1614–1617, 2008.
- [33] S. Haessler, T. Balčiunas, G. Fan, G. Andriukaitis, A. Pugžlys, A. Baltuška, T. Witting, R. Squibb, A. Zaïr, J. W. G. Tisch, J. P. Marangos, and L. E. Chipperfield. Optimization of quantum trajectories driven by strong-field waveforms. *Phys. Rev. X*, 4:021028, 2014.
- [34] S. De, I. Znakovskaya, D. Ray, F. Anis, Nora G. Johnson, I. a. Bocharova, M. Magrakvelidze, B. D. Esry, C. L. Cocke, I. V. Litvinyuk, and M. F. Kling. Field-Free Orientation of CO Molecules by Femtosecond Two-Color Laser Fields. *Physical Review Letters*, 103(15):1–4, 2009.
- [35] D. Ray, F. He, S. De, W. Cao, H. Mashiko, P. Ranitovic, K. P. Singh, I. Znakovskaya, U. Thumm, G. G. Paulus, M. F. Kling, I. V. Litvinyuk, and C. L. Cocke. Ion-Energy Dependence of Asymmetric Dissociation of D₂ by a Two-Color Laser Field. *Physical Review Letters*, 103(22):223201, 2009.
- [36] Li Zhang, Xinhua Xie, Stefan Roither, Yueming Zhou, Peixiang Lu, Daniil Kartashov, Markus Schöffler, Dror Shafir, Paul B. Corkum, Andrius Baltuška, André Staudte, and Markus Kitzler. Subcycle control of electron-electron correlation in double ionization. *Phys. Rev. Lett.*, 112:193002, 2014.
- [37] J. Wu, L. Schmidt, M. Kunitski, M. Meckel, S. Voss, H. Sann, H. Kim, T. Jahnke, a. Czasch, and R. Dörner. Multiorbital Tunneling Ionization of the CO Molecule. *Physical Review Letters*, 108(18):1–5, 2012.
- [38] Xinhua Xie, Katharina Doblhoff-Dier, Stefan Roither, Markus S. Schöffler, Daniil Kartashov, Huailiang Xu, Tim Rathje, Gerhard G. Paulus, Andrius Baltuška, Stefanie Gräfe, and Markus Kitzler. Attosecond-recollision-controlled selective fragmentation of polyatomic molecules. *Physical Review Letters*, 109:243001, 2012.
- [39] R. Dörner, V. Mergel, O. Jagutzki, J. Ullrich L. Spielberger, R. Moshhammer, and H. Schmidt-Böcking. Cold target recoil ion momentum spectroscopy: A ‘momentum microscope’ to view atomic collision dynamic. *Physics Reports*, 330:95–192, 2000.
- [40] J Ullrich, R Moshhammer, A Dorn, R Dörner, L Ph H Schmidt, and H Schmidt-Böcking. Recoil-ion and electron momentum spectroscopy: reaction-microscopes. *Reports on Progress in Physics*, 66(9):1463, 2003.
- [41] Bradley Moser and GN Gibson. Ultraslow dissociation of the h²⁺ molecular ion via two-color ultrafast laser pulses. *Physical Review A*, 80(4):041402, 2009.
- [42] J H Posthumus, J Plumridge, L J Frasinski, K Codling, E J Divall, A J Langley, and P F Taday. Slow protons as a signature of zero-photon dissociation of h²⁺ in intense laser fields. *Journal of Physics B: Atomic, Molecular and Optical Physics*, 33(16):L563, 2000.
- [43] P. B. Corkum. Plasma perspective on strong field multiphoton ionization. *Phys. Rev. Lett.*, 71:1994–1997, 1993.
- [44] Szczepan Chelkowski, André D. Bandrauk, and Alexander Apolonski. Phase-dependent asymmetries in strong-field photoionization by few-cycle laser pulses. *Physical Review A - Atomic, Molecular, and Optical Physics*, 70(1):13815, 2004.
- [45] Szczepan Chelkowski and André D Bandrauk. Asymmetries in strong-field photoionization by few-cycle laser

- pulses: Kinetic-energy spectra and semiclassical explanation of the asymmetries of fast and slow electrons. *Phys. Rev. A*, 71(5):53815, 2005.
- [46] Gennady Yudin and Misha Ivanov. Nonadiabatic tunnel ionization: Looking inside a laser cycle. *Physical Review A*, 64(1):6–9, 2001.
- [47] Michael Spanner, Jochen Mikosch, Arjan Gijsbertsen, Andrey E Boguslavskiy, and Albert Stolow. Multi-electron effects and nonadiabatic electronic dynamics in above threshold ionization and high-harmonic generation. *New Journal of Physics*, 13(9):093010, 2011.
- [48] Xinhua Xie, Katharina Doblhoff-Dier, Huailiang Xu, Stefan Roither, Markus S. Schöffler, Daniil Kartashov, Sonia Erattupuzha, Tim Rathje, Gerhard G. Paulus, Kaoru Yamanouchi, Andrius Baltuška, Stefanie Gräfe, and Markus Kitzler. Selective Control over Fragmentation Reactions in Polyatomic Molecules Using Impulsive Laser Alignment. *Physical Review Letters*, 112(16):163003, 2014.
- [49] Xinhua Xie, Stefan Roither, Markus Schöffler, Erik Lötstedt, Daniil Kartashov, Li Zhang, Gerhard G. Paulus, Atsushi Iwasaki, Andrius Baltuška, Kaoru Yamanouchi, and Markus Kitzler. Electronic Predetermination of Ethylene Fragmentation Dynamics. *Physical Review X*, 4(2):021005, 2014.